Configuration interaction calculations of low-lying electronic states of O_2,O_2^+, and O_2^{2+}

Nelson H. F. Beebe, Erik W. Thulstrup, and Andreas Andersen

Department of Chemistry, Aarhus University, DK-8000 Aarhus C., Denmark
(Received 5 September 1975)

Minimal basis full valence CI calculations of potential curves are reported for more than 300 low-lying states of O_2, O_2^+, and O_2^{2+}. A large number of new bound states of O_2^+ and some metastable states of O_2^{2+} are predicted, and from a comparison with known states of O_2 and O_2^+, predictions are made for the spectroscopic constants of the as yet experimentally unknown states.

INTRODUCTION

The oxygen molecule and its positive ions are of great interest to a wide range of chemists, physicists, and aeronomists. Very useful and easily applicable information on the electronic states of these systems is provided by the full potential curves. Such curves are known from experiments for a large number of the lower states of O_2, and for a small fraction of the low-lying states of O_2^+, whereas the information on the electronic states of O_2^{2+} (many of which are bound) is much less detailed. One of the foremost purposes of this work is to provide reliable information on potential curves of the many electronic states of the three systems, for which sufficient experimental information has not been obtained. The degree of accuracy of the theoretical data can be judged from a comparison of the calculated and experimental results for the experimentally well-known states, and from this comparison improved predictions can be obtained, since the deviation between theory and experiment ususally goes in one direction for each spectroscopic constant.

The potential curves of the negative ion, O_2^-, are also of great interest, particularly in connection with the study of resonances in electron impact on O_2 (see, e.g., Schulz).[1] Michels and Harris[2] have carried out calculations on O_2^- similar to those presented here, and Krauss *et al.*[2] have reported extensive and more accurate calculations on several states, so we have not included calculations on the negative ion.

CALCULATIONS

Part of the calculations were carried out with a program which has been previously described.[3] A newer version of the program developed by one of us (NHFB) was used for the Σ states, and some others were recalculated in regions of avoided crossings. The methods used are essentially the same in the two programs, but many technical improvements have speeded the calculations considerably. Particularly noteworthy are the use of list construction techniques for matrix elements and the density matrices. The lists contain all configuration dependence and integral indices and need be constructed only once for a given set of configurations. Subsequent points on the potential curves then require only computation of new integrals and solution of secular problems without further reference to the configurations. Matrix element construction from the lists is reduced to an insignificant amount of time relative to integral generation and secular problem solution. In the calculations reported here, we have computed from 15 to 20 points on the potential curves, extracting from five to ten roots of the secular problem at each point. For a 100 configuration calculation, typical timing for a single point is 70 sec for integrals and 30 sec for matrix elements, secular problems, and density matrices on a CDC 6400 computer (using 110K octal 60-bit words in fast core and an equivalent amount in slow core), resulting in a total expenditure of from 20 to 30 min for potential curves of a given symmetry. By saving integrals and reusing them for different symmetries, the time is cut to 5 to 10 min.

We perform full valence CI(VCI) calculations. With the molecular orbitals corresponding essentially to atomic 1*s* orbitals held fixed, all possible excitations of the proper symmetry are allowed within the limited basis set. The effect of freezing the core is completely negligible for *relative* energies, and decreases the number of configruations considerably. Minimal Slater type orbital (STO) bases were chosen according to procedures reported earlier[4]; the results correspond approximately to using the Clementi–Raimondi[5] rules on a system with one electron less than the system in question. Exponent optimization would of course be possible since the calculations are relatively inexpensive. However, our *ad hoc* procedure seems to give a reasonable balance, and in view of the fact that we are interested in obtaining a semiquantitative picture of a large number of states (more than 300 are reported here from 54 symmetries), we do not feel that the extra expense is justified. As mentioned above, our attitude is rather that by making comparison of our results with those obtained from experiment, we can obtain a measure of confidence about the reliability of the predictions for as yet experimentally unknown states.

As an indication of the cost of improving the results,

TABLE I. STO exponents. All m_l components of the *p* type STO's are included in the basis.

	O_2	O_2^+	O_2^{2+}
1*s*	7.6579	7.6579	7.6579
2*s*	2.28	2.36	2.44
2*p*	2.28	2.36	2.44

TABLE II. The number of configurations used in the calculations. For Σ symmetries, the figures given represent the numbers of linearly independent configurations after performing the reflection symmetry projections.

State	O_2	O_2^{2+}	State	O_2^+
$^1\Sigma_g^+$	37	96	$^2\Sigma_{g,u}^+$	72
$^1\Sigma_g^-$	13	56	$^2\Sigma_{g,u}^-$	60
$^1\Sigma_u^+$	26	80	$^2\Pi_{g,u}$	109
$^1\Sigma_u^-$	18	64	$^2\Delta_{g,u}$	58
$^1\Pi_{g,u}$	36	120	$^2\Phi_{g,u}$	17
$^1\Delta_g$	22	74	$^4\Sigma_{g,u}^+$	28
$^1\Delta_u$	18	68	$^4\Sigma_{g,u}^-$	46
$^3\Sigma_g^+$	24	84	$^4\Pi_{g,u}$	57
$^3\Sigma_g^-$	30	108	$^4\Delta_{g,u}$	26
$^3\Sigma_u^+$	28	100	$^6\Sigma_{g,u}^+$	4
$^3\Sigma_u^-$	28	100	$^6\Sigma_{g,u}^-$	6
$^3\Pi_{g,u}$	44	164		
$^3\Delta_g$	18	82		
$^3\Delta_u$	20	88		

we note that Stevens *et al.*[6] have recently reported a single potential curve for OH in near-perfect agreement with experiment. They used a large basis set and the multiconfiguration SCF method, using about 60 min per point on an IBM 360/75. Since the latter is about five times faster than the CDC 6400, analogous calculations on these systems would require about 70 h for a single potential curve on our machine, or more than a year for all the states obtained here.

We report in Table I the STO bases used and in Table II the number of configurations for each symmetry. In addition to spin orbital angular momentum and inversion symmetry projections, our new program also carries out reflection symmetry projections for the Σ states. This halves the size of the secular problems to be considered, but necessitates orthonormalization of the configuration lists since linear dependencies arise when two configurations have the same reflection projection. The figures in Table II refer to the number of linearly independent configurations obtained, and the number of configurations before the reflection projection is the sum of the + and − sets.

TABLE III. O_2 molecular states arising from separated atom states.

$O(^3P)+O(^3P)$	$^1\Sigma_g^+(2)$, $^1\Sigma_u^-$, $^1\Pi_{g,u}$, $^1\Delta_g$, $^3\Sigma_g^-$, $^3\Sigma_u^+(2)$, $^3\Pi_{g,u}$, $^3\Delta_u$, $^5\Sigma_g^+(2)$, $^5\Sigma_u^-$, $^5\Pi_{g,u}$, $^5\Delta_g$,
$^3P+^1D$	$^3[\Sigma^+, \Sigma^-(2), \Pi(3), \Delta(2), \Phi]_{g,u}$
$^1D+^1D$	$^1\Sigma_g^+(3)$, $^1\Sigma_u^-(2)$, $^1\Pi_{g,u}(2)$, $^1\Delta_g(2)$, $^1\Delta_u$, $^1\Phi_{g,u}$, $^1\Gamma_g$
$^3P+^1S$	$^3[\Sigma^-, \Pi]_{g,u}$
$^1D+^1S$	$^1[\Sigma^+, \Pi, \Delta]_{g,u}$
$^1S+^1S$	$^1\Sigma_g^+$
$^3P+^5S^\circ$	$^{1,3,5,7}[\Sigma^+, \Pi]_{g,u}$
$^1D+^5S^\circ$	$^5[\Sigma^-, \Pi, \Delta]_{g,u}$

TABLE IV. Calculated and experimental separated atom limits for O_2.

	E_{calc}^{total} (Hartrees)	E_{calc}^{rel} (eV)	E_{exp}^{rel} (eV)
$O(^3P)+O(^3P)$	−149.0671600	0	0
$^3P+^1D$	−148.9709725	2.617	1.970
$^3P+^1S$	−148.8880852	4.873	4.190
$^1D+^1D$	−148.8747850	5.235	3.940
$^1D+^1S$	−148.7918977	7.490	6.160
$^1S+^1S$	−148.7090103	9.746	8.381

We discuss each of the molecules separately in the following sections, but some general remarks are in order here. Rather than present a table of several thousand energies, we report only plots of the curves here. The energy tables are of much less interest, but have been deposited with the NAPS data depository.[7] The plots were generated by carrying out a linear polynomial spline interpolation of the computed curves to produce a dense grid suitable for computer plotting of smooth curves. The classic treatise on splines is the book by Ahlberg *et al.*,[8] but for our purposes, the relevant information is that it is possible to fit polyno-

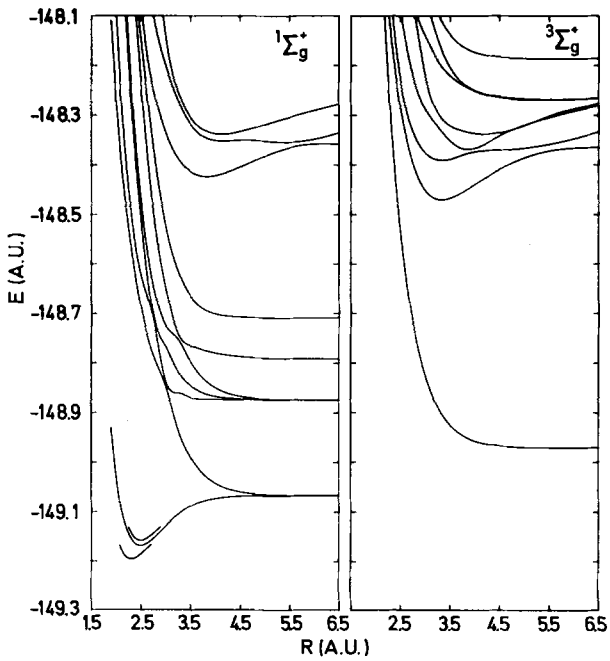

FIG. 1. Calculated O_2 $^{1,3}\Sigma_g^+$ potential curves. The lower partial curve is the experimental RKR curve (Ref. 20) at the experimental r_e value, while in the upper partial curve, it has been shifted to the calculated r_e value.

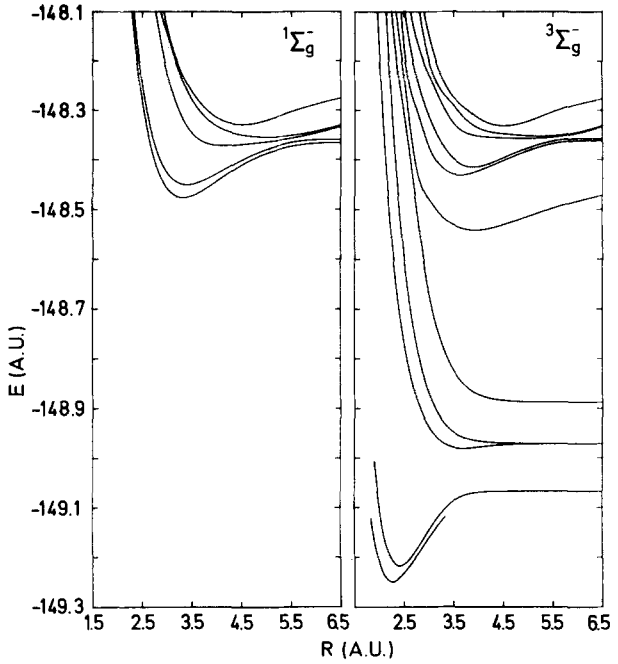

FIG. 2. Calculated O_2 $^{1,3}\Sigma_g^-$ potential curves. The partial curve is the experimental RKR curve (Ref. 20).

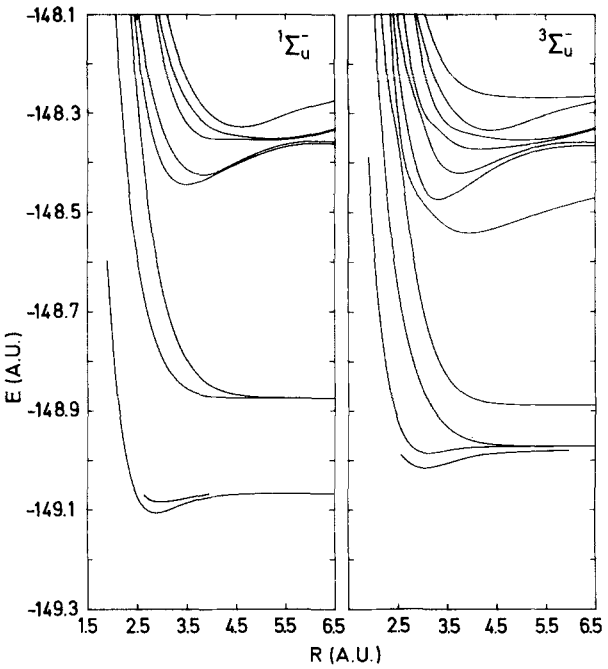

FIG. 4. Calculated O_2 $^{1,3}\Sigma_u^-$ potential curves. See note on Fig. 2.

mials of degree $2n-1$ between adjacent points, joining the polynomial segments by requiring that the derivatives of order 1, 2, . . . , $2n-2$ match at the common point and that the polynomials are exact at both ends of the segments. Additional conditions are necessary at the two outer points; the so-called "type II" boundary conditions have proved most satisfactory here. They involve setting the derivatives of order $n, n+1, \ldots,$ $2n-2$ to zero at the boundaries. The spline fits have several advantages. First, the smooth interpolation makes possible rapid computerized production of plots, eliminating both the tedium and "artistic" prejudices of hand-drawn curves. Second, the interpolating function passes *exactly* through the data points, which is not true with least-squares fits. Third, no drastic assumptions about the functional form (other than smoothness and single valuedness) are required; the spline fit works for bound, humped, and repulsive po-

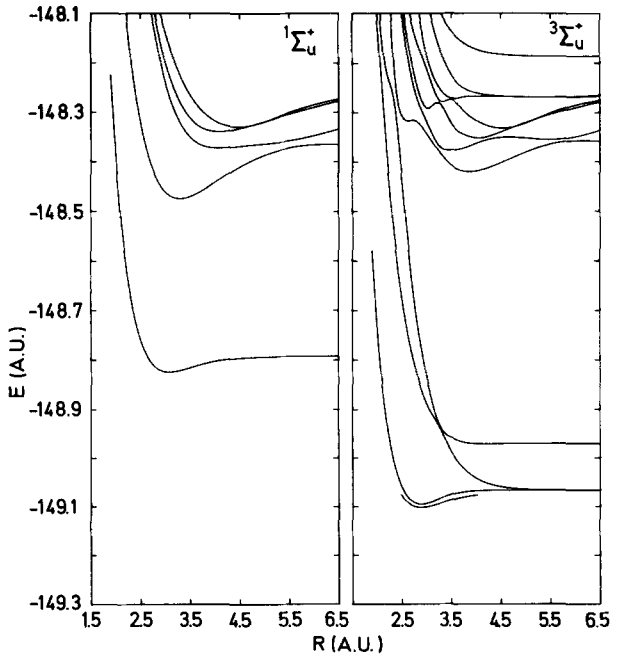

FIG. 3. Calculated O_2 $^{1,3}\Sigma_u^+$ potential curves. See note on Fig. 2.

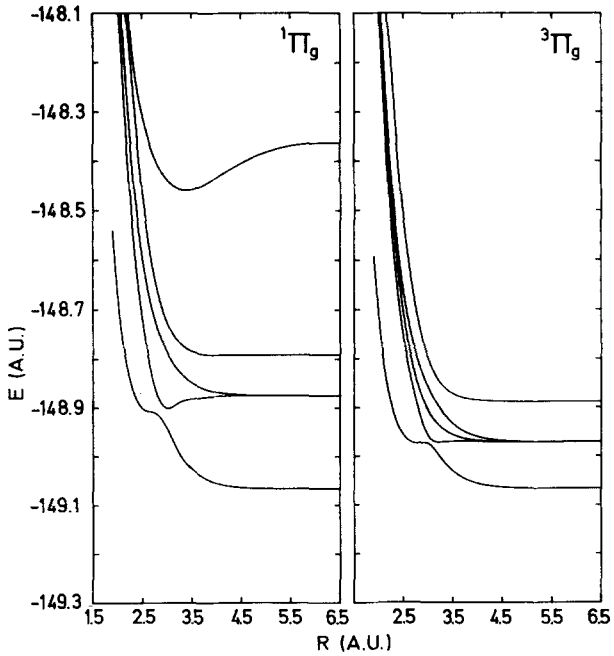

FIG. 5. Calculated O_2 $^{1,3}\Pi_g$ potential curves.

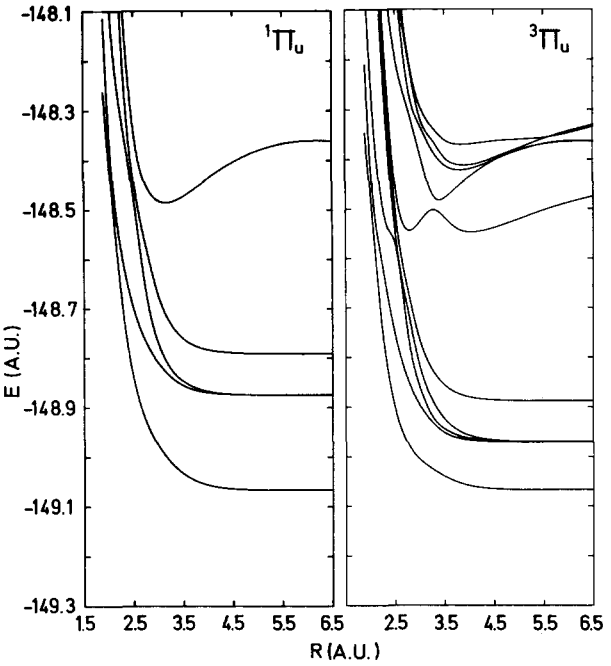

FIG. 6. Calculated O_2 $^{1,3}\Pi_u$ potential curves.

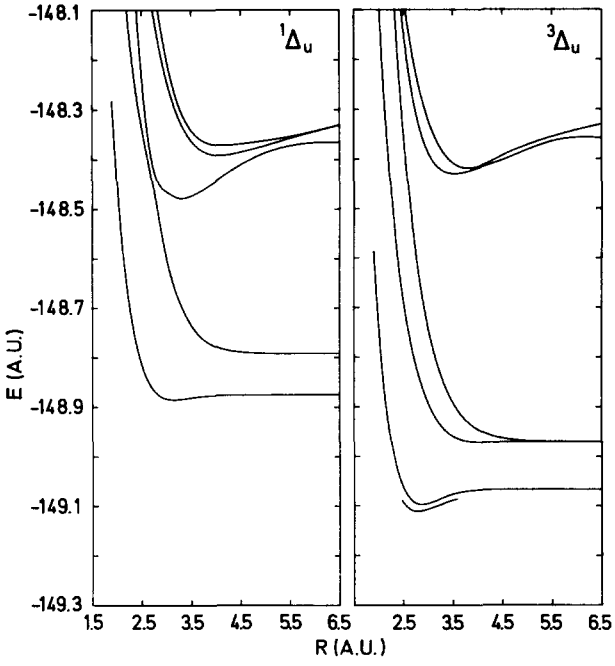

FIG. 8. Calculated O_2 $^{1,3}\Delta_u$ potential curves. See note on Fig. 2.

tential curves, as well as innumerable other functions, such as molecular properties. Fourth, the polynomial representation makes possible a conversion to the Dunham expansion[9] for bound potential curves in order to obtain estimates of spectroscopic constants.

We have programmed the general $2n-1$ degree spline polynomial interpolation and have investigated various degrees for the interpolation. The possibility of prediction of spectroscopic constants from the spline polynomial was of particular interest of us. The process of going from spectroscopic constants to an assumed functional form of the potential curve has been reviewed extensively by Varshni[10] and by Steele *et al.*[11] We have here the reverse process. In previous work, the Hulburt–Hirschfelder modification to the Morse curve[12] (HHM) was used, after we had decided that it was about the best of the available functional forms. The HHM curve requires a nonlinear least-squares fit, which is both time consuming and difficult to find a satisfactory parameter set for. In addition, deviations of up to 0.1 eV at the data points have often resulted, even after extensive parameter searches. The spline fits completely eliminate both the time and the search problem since the spline polynomial coefficients can be obtained by solution of a large, but banded, equation system.

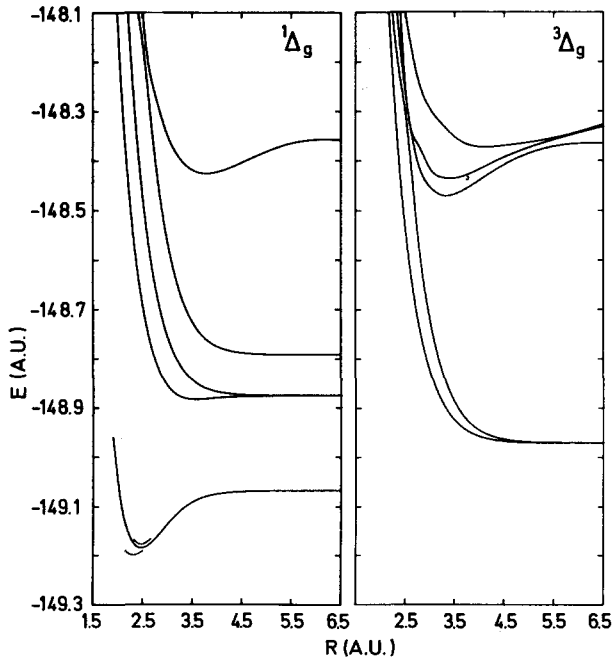

FIG. 7. Calculated O_2 $^{1,3}\Delta_g$ potential curves. See note on Fig. 1.

TABLE V. Spectroscopic parameters for calculated and observed states of O_2. Experimental values are given in parenthesis.

State	T_e (eV)	r_e (Å)	ω_e (cm^{-1})	D_e (eV)
$X\,^3\Sigma_g^-$	0.00 (0.00)	1.278 (1.208)	1673 (1580)	4.11 (5.21)
$a\,^1\Delta_g$	0.92 (0.98)	1.299 (1.216)	1505 (1509)	3.20 (4.23)
$b\,^1\Sigma_g^+$	1.36 (1.64)	1.317 (1.227)	1378 (1433)	2.75 (3.58)
$c\,^1\Sigma_u^-$	3.05 (4.10)	1.529 (1.517)	948 (794)	1.06 (1.11)
$C\,^3\Delta_u$	3.28 (4.31)	1.520 (1.5)	990 (~750)	0.83 (0.91)
$A\,^3\Sigma_u^+$	3.33 (4.39)	1.525 (1.522)	977 (799)	0.78 (0.82)
$B\,^3\Sigma_u^-$	6.34 (6.17)	1.648 (1.604)	697 (709)	0.38 (1.01)
$^1\Delta_u$	9.06 (~10.9)	1.666 (~1.2)	641	0.28
$^1\Pi_u$	12[a] (11)	(1.19)		

[a] Calculated vertical excitation energy ($R = 1.278$ Å) for our repulsive $^1\Pi_u$ state (see Fig. 6).

TABLE VI. Predicted unobserved bound states of O_2.

State	T_e (eV)	r_e (Å)	ω_e (cm^{-1})	D_e (eV)
$^3\Sigma_g^-(2)$	6.45	1.947	553	0.27
$^1\Pi_g(2)$	8.62	1.601	1690	0.73
$^1\Delta_g(2)$	9.14	1.886	457	0.20
$^1\Sigma_u^+$	10.72	1.633	776	0.88
$^1\Sigma_g^-$	20.17	1.757	932	2.95
$^1\Sigma_u^+(2)$	20.22	1.752	894	2.92
$^3\Sigma_g^+$	20.37	1.764	916	2.78
$^1\Sigma_g^-(2)$	20.88	1.797	832	2.36

In our opinion, the semiclassical Rydberg–Klein–Rees method is the most satisfactory method of obtaining potential curves for experiment. Although it cannot be used for predicting a full potential curve from knowledge of a few vibrational levels, it can reasonably often predict a limited extrapolation above the highest known vibrational level. Within the Born–Oppenheimer approximation, it can be regarded as essentially the "exact" experimental curve. Zare[13] has shown that the RKR curve for I_2, when used as the potential energy in the vibrational Schrödinger equation, yields vibrational energies which agree to within 10^{-6} cm^{-1} of those used to calculate the RKR curve. Since experimental accuracy is seldom better than 0.01 cm^{-1}, the RKR curve may thus be considered "self-consistent." Therefore, in order to test spline fit predictions of spectroscopic constants, we have computed RKR curves for the known states of O_2 and O_2^+ using the method proposed by Zeleznik[14] which analytically removes the singularity in the RKR integrals. We have checked these results with the RKR integration method recently given by Tellinghuisen[15]; minor deviations of 0.0005 Å in the turning points occur at high vibrational levels, but can be considered completely insignificant. Spline fits of orders 3, 5, 7, ..., 21 were carried out for the RKR curves of several states of O_2 and O_2^+. Orders larger than 5 were found to give unphysical fluctuations between the data points and are therefore unsatisfactory for both interpolation and calculation of spectroscopic constants. Orders 3 and 5 were about equally satisfactory, and the results indicate that one can expect about 10% accuracy in predicted ω_e and α_e values, B_e is reliable to 0.001 cm^{-1}, and r_e to 0.001 Å. Predicted $\omega_e x_e$ values are typically from 50% to 400% too large. According to the Dunham relations,[9] the internuclear distance at the minimum of the potential curve, r_{min}, differs from the r_e value derived from B_e by small second-order terms. For all the cases presented here, the two values differ by 0.0001 Å or less, so that to the accuracy of the spline fits, they may be considered identical. In the tables, we have therefore reported only ω_e and r_e values obtained from third-order spline fits of our calculated data, and the reader should remember that the ω_e values are only rather course estimates. One could of course use the spline interpolated curves in the vibrational Schrödinger equation to obtain vibrational constants from the computed levels. However, in view of the accuracy of our curves, we have not found such effort worthwhile. Instead, we have plotted the known RKR curves along with our interpolated curves so that the reader may obtain a visual impression of the reliability of our calculations.

TABLE VIII. Calculated and experimental separated atom limits for O_2^+.

	E_{calc}^{total} (Hartrees)	E_{calc}^{rel} (eV)	E_{exp}^{rel} (eV)
$O(^3P)+O(^4S^o)$	−148.7121231	0	0
$^1D+^4S^o$	−148.6125606	2.709	1.9673
$^3P+^2D^o$	−148.5627794	4.064	3.3249
$^1S+^4S^o$	−148.5277595	5.017	4.1896
$^3P+^2P^o$	−148.5081366	5.551	5.0171
$^1D+^2D^o$	−148.4632169	6.773	5.2922

THE O_2 MOLECULE

The oxygen molecule has been theoretically studied by several authors,[16–18] the work of Schaefer and Harris[19] on 62 low-lying states of O_2 being the most ex-

TABLE VII. O_2^+ molecular states arising from separated atom limits.

$O(^3P)+O^+(^4S^o)$	$^{2,4,6}[\Sigma^+, \Pi]_{g,u}$
$^1D+^4S^o$	$^4[\Sigma^-, \Pi, \Delta]_{g,u}$
$^3P+^2D^o$	$^{2,4}[\Sigma^+(2), \Sigma^-, \Pi(3), \Delta(2), \Phi]_{g,u}$
$^1S+^4S^o$	$^4\Sigma_{g,u}^-$
$^3P+^2P^o$	$^{2,4}[\Sigma^+, \Sigma^-(2), \Pi(2), \Delta]_{g,u}$
$^1D+^2D^o$	$^2[\Sigma^+(2), \Sigma^-(3), \Pi(4), \Delta(3), \Phi(2), \Gamma]_{g,u}$
$^1D+^2P^o$	$^2[\Sigma^+(2), \Sigma^-, \Pi(3), \Delta(2), \Phi]_{g,u}$
$^1S+^2D^o$	$^2[\Sigma^-, \Pi, \Delta]_{g,u}$
$^5S^o+^4S^o$	$^{2,4,6,8}\Sigma_{g,u}^+$
$^1S+^2P^o$	$^2[\Sigma^+, \Pi]_{g,u}$

TABLE IX. Calculated spectroscopic constants for bound states of O_2^+. Experimental values are given in parenthesis.

State	T_e (eV)	r_e (Å)	ω_e (cm^{-1})	D_e (eV)
$X\,^2\Pi_g$	0.00 (0.00)	1.214 (1.117)	1691 (1905)	6.21 (6.78)
$a\,^4\Pi_u$	2.75 (4.09)	1.413 (1.382)	1289 (1036)	3.45 (2.69)
$A\,^2\Pi_u$	3.74 (4.99)	1.452 (1.408)	1083 (898)	2.46 (1.76)
$b\,^4\Sigma_g^-$	5.43 (6.12)	1.320 (1.280)	1281 (1187)	3.51 (2.60)
$^2\Phi_u$	5.75 (6.6)	1.414 (1.4)	1300 (900)	4.53 (3.5)
$^2\Delta_g$	6.90 (7.67)	1.364 (1.33)	1165 (930)	3.31 (2.44)
$B\,^2\Sigma_g^-$	7.71 (8.30)	1.324 (1.30)	1248 (1156)	2.56 (1.83)
$^2\Pi_u$	(12.0)			
$c\,^4\Sigma_u^-$	12.5 (12.42)	1.21 (1.18)	... (1540)	

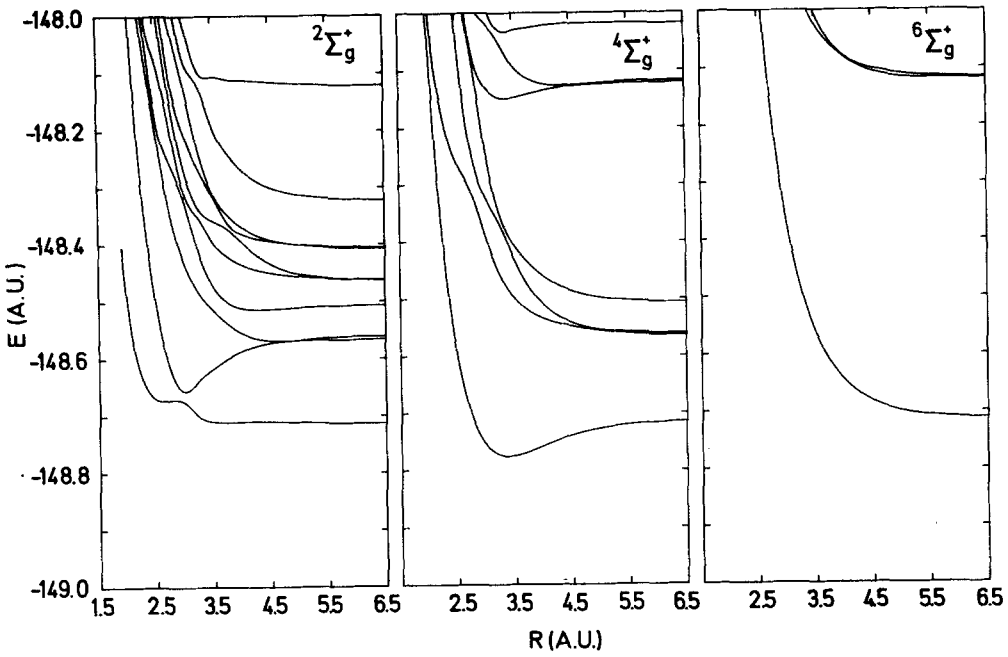

FIG. 9. Calculated $O_2^{+\,2,4,6}\Sigma_g^+$ potential curves.

tensive. Their work is very similar to ours, the main difference being the STO basis, which in their work was chosen from an optimized atomic basis for $O\,^3P$. The calculations in Ref. 19 include the states of primary interest in O_2. We have principally repeated the work by Schaefer and Harris on these states to compare the effect of different basis sets. We present in Table III the low-lying states of O_2 and their atomic state limits, in Table IV the calculated and experimetal dissociation limits, and in Figs. 1–8, the calculated potential curves. The dissociation limits were calculated in our program by carrying out a calculation with only 1-center integrals included, corresponding to $R=\infty$, using the same configurations as on the remainder of the potential curves. In the cases discussed by Schaefer and Harris, our results lead to essentially the same conclusions, and we therefore refer the reader to their discussion. The good agreement between the two calculations indicates the relative stability of a minimal basis calculation toward small changes in the

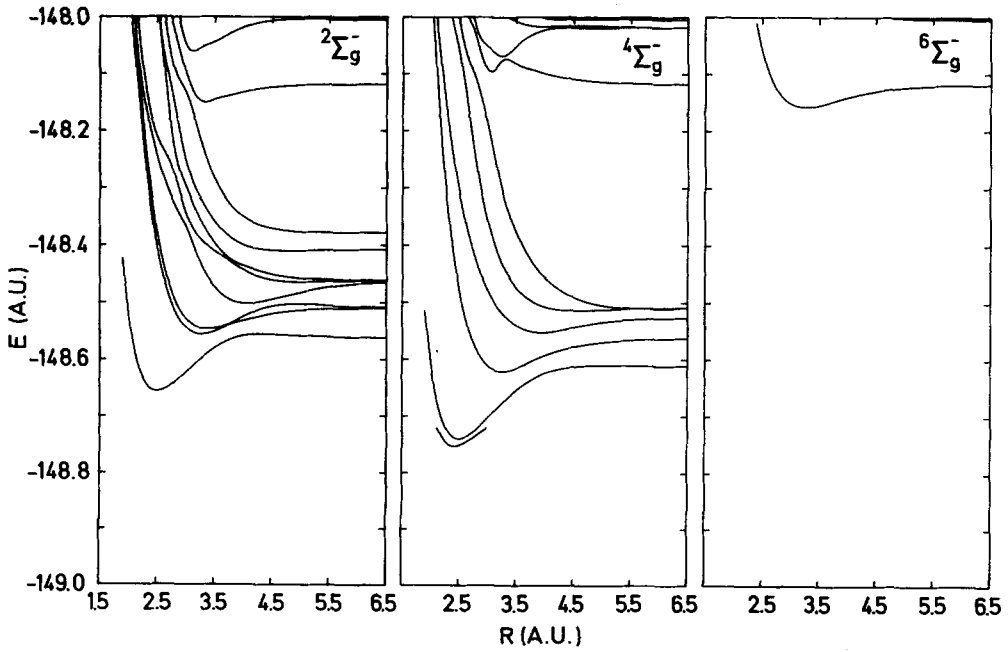

FIG. 10. Calculated $O_2^{+\,2,4,6}\Sigma_g^-$ potential curves. See note on Fig. 2.

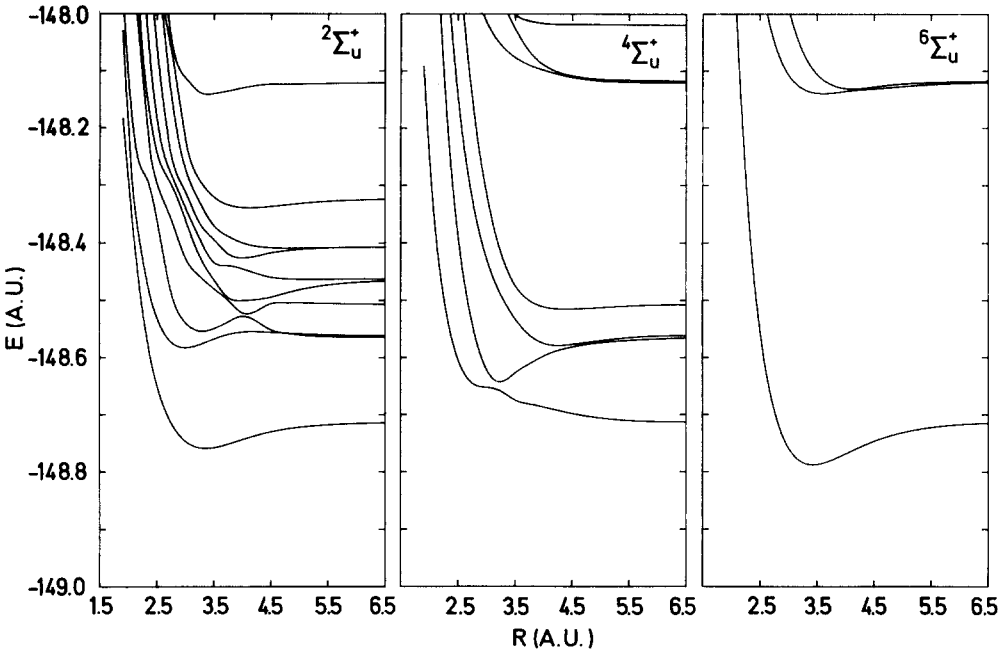

FIG. 11. Calculated $O_2^{+\,2,4,6}\Sigma_u^+$ potential curves.

orbital exponents.

Krupenie[20] has recently treated the spectra of oxygen and its ions in an excellent review, and we shall refer the reader to it for references to most of the work prior to 1971. At the time of Schaefer and Harris' work in 1968, seven bound non-Rydberg states of O_2, namely $X\,^3\Sigma_g^-$, $a\,^1\Delta_g$, $b\,^1\Sigma_g^+$, $c\,^1\Sigma_u^-$, $C\,^3\Delta_{ui}$, $A\,^3\Sigma_u^+$, and $B\,^3\Sigma_u^-$, were known. Of these, the C state is known only for $v=0$, 5, and 6, and the relative ordering of the c and C states had been somewhat uncertain. The calculations of Schaefer and Harris as well as ours predict $c\,^1\Sigma_u^-$ lower than $C\,^3\Delta_{ui}$ lower than $A\,^3\Sigma_u^+$, and this seems now to have been experimentally established.[20] All seven states are found to be bound in the calculations. We have plotted in Figs. 1–4, 7, and 8 the experimental RKR curves for these states. Since our calculated r_e values tend to be too large, we have plotted the RKR curves twice in some of the figures. The lower one corresponds to experiment, while the upper one has been moved to our calculated r_e values in order to obtain a better visual comparison of the shapes of the curves. The vertical energy scale for the RKR curves has not been adjusted to their T_e values. Calculated

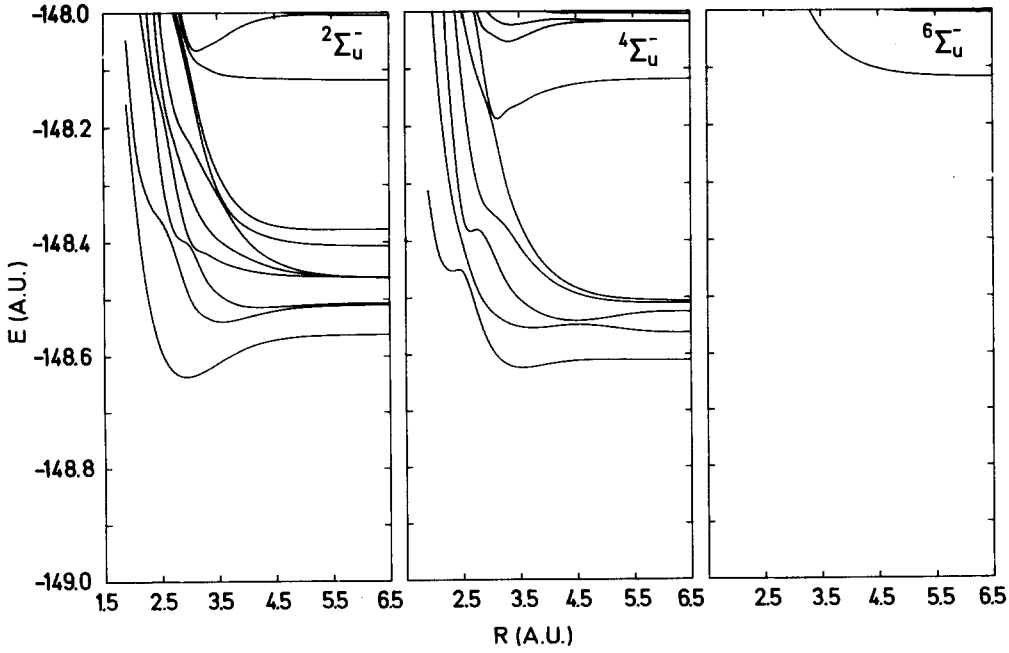

FIG. 12. Calculated $O_2^{+\,2,4,6}\Sigma_u^-$ potential curves.

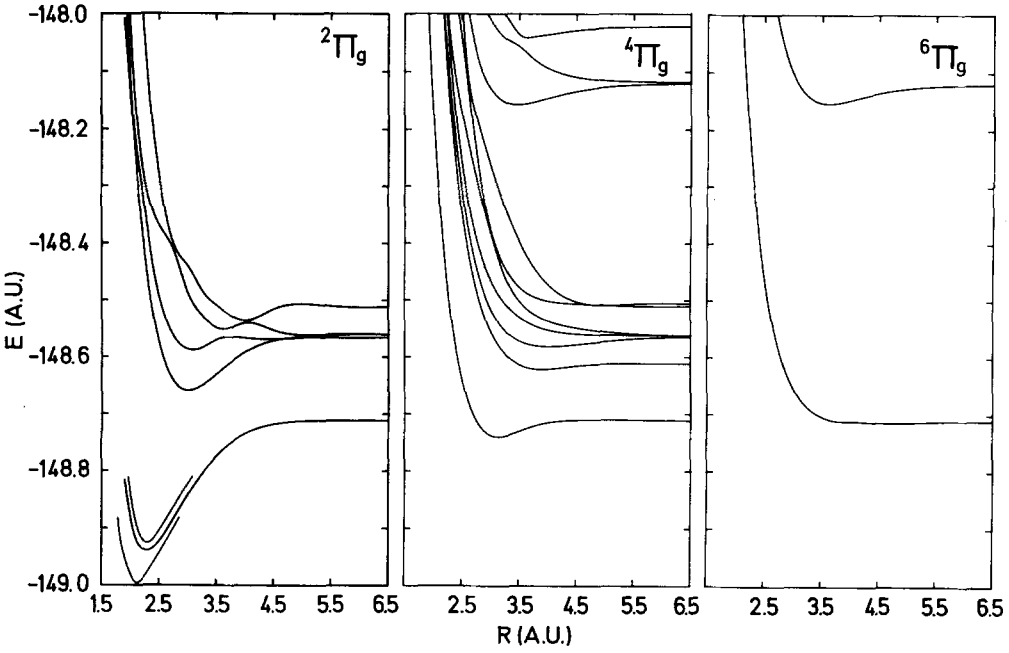

FIG. 13. Calculated $O_2^{+\,2,4,6}\Pi_g$ potential curves. See note on Fig. 1.

and experimental spectroscopic constants are given in Table V, and in Table VI calculated spectroscopic constants are given for states so far not observed. Considering the simplicity of these calculations, the agreement between the calculated and the RKR curves (except possibly for $c\,^1\Sigma_u^-$) is quite remarkable.

From the data in Table V it is clear that the deviations of calculated numbers from the experimental ones are partly systematic (e.g., all calculated r_e's are too high). This might make better predictions possible than the calculated numbers in Table VI, but in the O_2 case we have not found the systematics in the deviations sufficient for such a procedure. In the discussion of O_2^+, for which reliable predictions of unobserved states are badly needed, we have attempted such estimates.

Since 1968, five additional bound states, $\beta\,^3\Sigma_u^+$, $\alpha\,^1\Sigma_u^+$, $^3\Sigma_u^+$, $^1\Delta_u$, and $^1\Pi_u$ have been tentatively identified in experiments. In addition to the seven bound states known earlier, the calculations predict additional bound $^3\Sigma_g^-$, $^1\Pi_g$, $^1\Delta_u$, $^1\Delta_g$, and $^1\Sigma_u^+$ states. The experimental identification of the $^1\Pi_u$ state came from the measure-

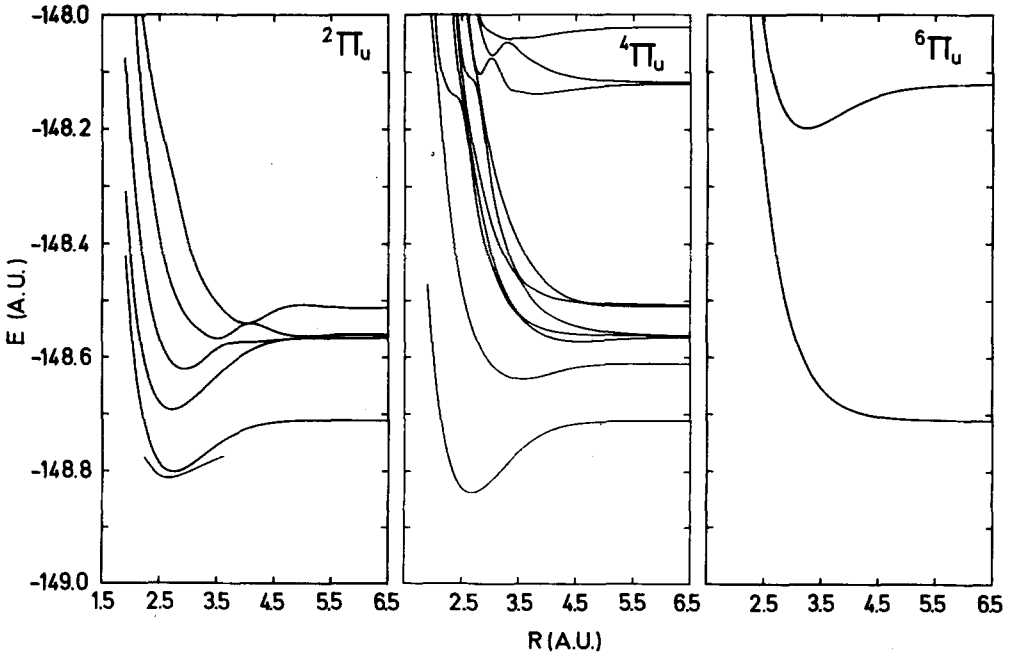

FIG. 14. Calculated $O_2^{+\,2,4,6}\Pi_u$ potential curves. See note on Fig. 2.

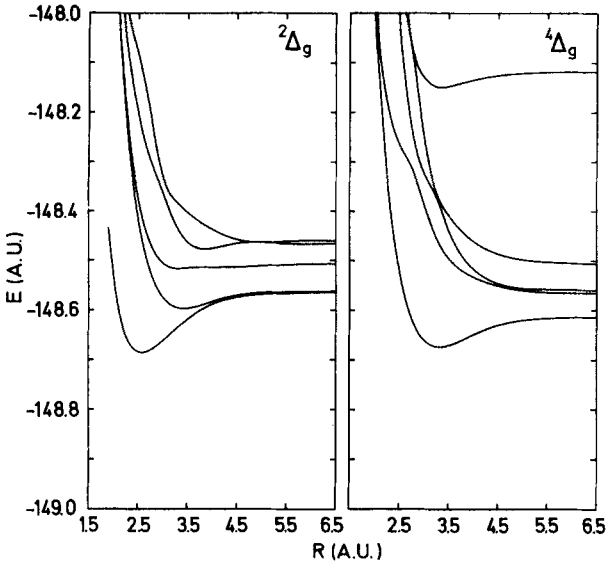

FIG. 15. Calculated $O_2^{+\,2,4}\Delta_g$ potential curves.

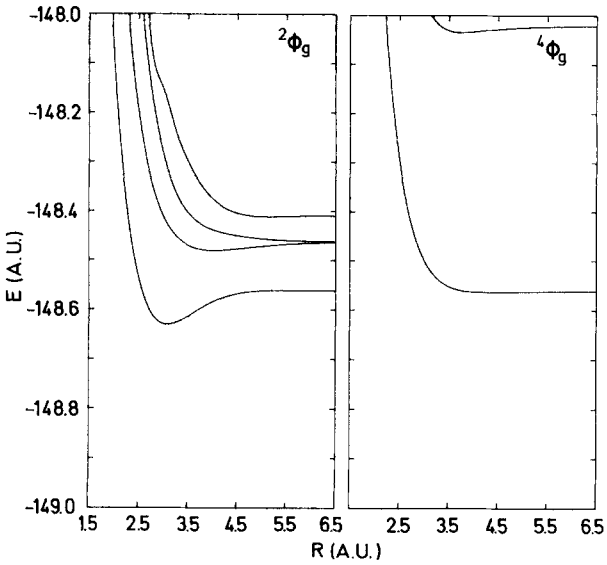

FIG. 17. Calculated $O_2^{+\,2,4}\Phi_g$ potential curves.

ment of the absorption spectrum from the $a\,^1\Delta_g$ state. The rotational structure, found only from $v=0$ in both upper and lower states, indicated that a perturbed $^1\Pi$ state was involved, and because the absorption was fairly strong, u symmetry was assumed. Our calculations indicate that both $^1\Pi_g$ and $^1\Pi_u$ states lie at about the right position above $a\,^1\Delta_g$. However, the u state is smoothly repulsive, while the g state has a distinct avoided crossing (Figs. 5 and 6). A small well here is quite possible (see discussion on the c state of O_2^+ in the next section), and would explain the perturbations and the observation of only the $v=0$ transition. Assignment of the upper state as $^1\Pi_g$ would involve a parity forbidden transition, but similarly forbidden transitions $a \rightarrow X$, $b \rightarrow X$, and $b \rightarrow a$ are well-known in O_2. The new $^1\Delta_u$ state is predicted to lie about 9 eV above the X state (T_e value); experimentally it is found at 10.94 eV. The remaining three new observed states noted above are all characterized as Rydberg states because of the close similarity of their rotational constants and ω_e values to those of $O_2^+ X\,^2\Pi_g$. Since our basis set does not include diffuse orbitals, we should not expect to find such states, and do not. The bound $^1\Sigma_u^+$ that we do find is somewhat higher than our lowest $^1\Delta_u$; its apparent lack of Rydberg character is almost certainly due to the limited basis employed. Transitions to the predicted bound state $^3\Sigma_g^-$ (2) would only be allowed from the $B\,^3\Sigma_u^-$ state among the lowest seven bound states, and because these two have rather different r_e values and also go to the same separated atom limit, it is not surprising that this state has not been observed. The $^1\Delta_g$(2) state predicted bound by the calculations cannot be reached from any of the lower states by allowed transitions.

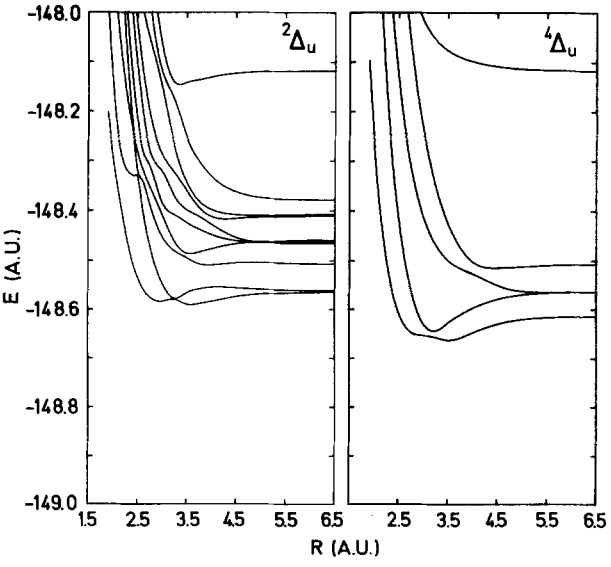

FIG. 16. Calculated $O_2^{+\,2,4}\Delta_u$ potential curves.

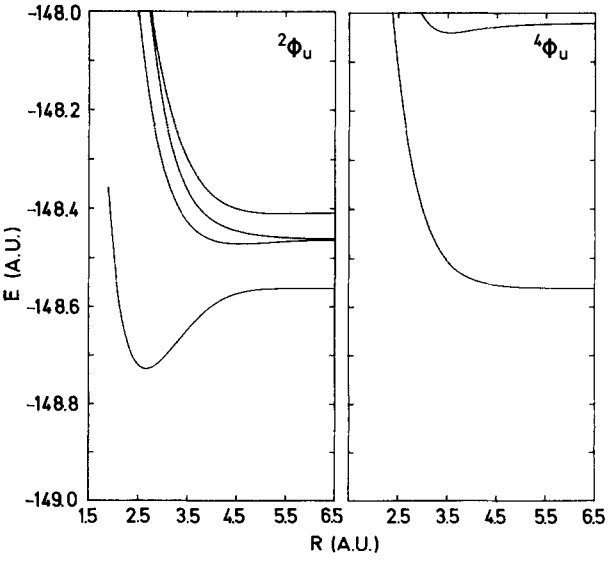

FIG. 18. Calculated $O_2^{+\,2,4}\Phi_u$ potential curves.

TABLE X. Predicted spectroscopic constants for bound excited states of O_2^+. The constants have been adjusted by the corrections noted in the text, and experimental values are given in parenthesis.

State	T_e (eV)	r_e (Å)	ω_e (cm^{-1})	D_e (eV)
$a\,^4\Pi_u$	3.65 (4.09)	1.378 (1.382)	1119 (1036)	2.60 (2.69)
$A\,^2\Pi_u$	4.64 (4.99)	1.417 (1.408)	913 (898)	1.61 (1.76)
$^6\Sigma_u^+(1)$	5.03	1.778	663	1.15
$^4\Sigma_g^+(1)$	5.37	1.754	607	0.83
$^2\Sigma_u^+(1)$	5.81	1.743	522	0.39
$b\,^4\Sigma_g^-(1)$	6.33 (6.12)	1.285 (1.280)	1121 (1197)	2.66 (2.60)
$^2\Phi_u$	6.65 (6.6)	1.379 (1.4)	1130 (900)	3.68 (3.5)
$^2\Pi_u(2)$	7.60	1.403	1010	2.66
$^2\Delta_g$	7.80 (7.67)	1.329 (1.33)	995 (930)	2.46 (2.44)
$^4\Delta_g$	8.12	1.721	665	0.78
$^4\Delta_u$	8.42	1.830	674	0.49
$^2\Pi_g$	8.50	1.561	973	1.77
$B\,^2\Sigma_g^-$	8.61 (8.30)	1.289 (1.30)	1078 (1150)	1.71 (1.83)
$^2\Sigma_g^+(2)$	8.61	1.553	1750	1.65
$^4\Sigma_u^+(2)$	8.97	1.676	1354	1.28
$^2\Sigma_u^-$	9.15	1.522	825	1.17
$^2\Phi_g$	9.31	1.610	822	1.01
$^2\Pi_u(3)$	9.54 (vert. 12)	1.517	957	0.78
$^4\Sigma_g^-(2)$	9.56	1.685	727	0.75
$^2\Delta_g(2)$	10.21	1.776	558	0.11
$^2\Sigma_g^-(2)$	11.34	1.700	713	0.41
$^2\Sigma_g^-(3)$	11.60	1.751	? (humped)	0.19
$^2\Sigma_g^-(4)$	12.81	2.116	473	0.14
$^6\Sigma_g^-(1)$	22.17	1.678	505	0.22

Finally, we note that the avoided crossings found by Schaefer and Harris on the $^3\Pi_u$ curves are clearly seen in Fig. 6, and are also clearly evident in the $^1\Sigma_g^+$, $^3\Sigma_u^+$, $^1\Pi_g$, $^3\Pi_g$, and $^3\Pi_u$ states dissociating to low-lying atomic atomic limits.

Schaefer[21] has re-examined the X state with a larger basis set and a "first-order" CI wavefunction, obtaining somewhat improved spectroscopic parameters.

TABLE XI. O_2^{2+} molecular states arising from separated atom states.

$O^+(^4S^o)+O^+(^4S^o)$	$^{1,5}\Sigma_g^+$, $^{3,7}\Sigma_u^+$
$^4S^o+^2D^o$	$^{3,5}[\Sigma,\ \Pi,\ \Delta]_{g,u}$
$^4S^o+^2P^o$	$^{3,5}[\Sigma^-,\ \Pi]_{g,u}$
$^2D^o+^2D^o$	$^1[\Sigma_g^+(3),\ \Sigma_u^-(2),\ \Pi_g(2),\ \Pi_u(2),\ \Delta_g(2),\ \Delta_u,\ \Phi_{g,u},\ \Gamma_g]$
	$^3[\Sigma_u^+(3),\ \Sigma_g^-(2),\ \Pi_u(2),\ \Pi_g(2),\ \Delta_u(2),\ \Delta_g,\ \Phi_{g,u},\ \Gamma_u]$
$^2D^o+^2P^o$	$^{1,3}[\Sigma^+,\ \Sigma^-(2),\ \Pi(3),\ \Delta(2),\ \Phi]_{g,u}$
$^2P^o+^2P^o$	$^1\Sigma_g^+(2)$, $^1\Sigma_u^-$, $^1\Pi_g$, $^1\Pi_u$, $^1\Delta_g$, $^3\Sigma_u^+(2)$, $^3\Sigma_g^-$, $^3\Pi_g$, $^3\Pi_u$, $^3\Delta_u$
$^4S^o+^4P$	$^{1,3,5,7}[\Sigma^+,\ \Pi]_{g,u}$
$^2D^o+^4P$	$^{3,5}[\Sigma^+(2),\ \Sigma^-,\ \Pi(3),\ \Delta(2),\ \Phi]_{g,u}$
$^2P^o+^4P$	$^{3,5}[\Sigma^+,\ \Sigma^-(2),\ \Pi(2),\ \Delta]_{g,u}$

TABLE XII. Calculated and experimental separated atom limits for O_2^{2+}.

	E_{calc}^{total} (Hartrees)	E_{calc}^{rel} (eV)	E_{exp}^{rel} (eV)
$O^+(^4S^o)+O^+(^4S^o)$	−148.4398450	0	0
$^4S^o+^2D^o$	−148.2854387	4.201	3.3249
$^4S^o+^2P^o$	−148.1310325	8.403	5.0171
$^2D^o+^2D^o$	−148.0754549	9.915	6.6498
$^2D^o+^2P^o$	−148.0733174	9.973	8.3420

Using the same technique and same basis set, Schaefer and Miller[22] investigated the much discussed predissociation of the B state, finding that it is crossed on the inner limb by the $^3\Pi_u$ and on the outer limb by $^1\Pi_u$, both repulsive states arising from a lower atomic limit. These results are in agreement with the earlier Schaefer and Harris work and with our calculations. Peyerimhoff and Buenker[23] investigated the $X\,^3\Sigma_g^-$, $a\,^1\Delta_g$, and $b\,^1\Sigma_g^+$ states with CI wavefunctions having configuration selections optimized at each point on the curves, (from 150 to 500 CI) using larger basis sets and natural orbital iterations in an attempt to get accurate predictions of D_e and r_e. While optimization of the wavefunction by varying the configuration selection at each point can lead to improved results, it clearly becomes impractical if many states are to be investigated, and, what is more, the advantage of the list construction technique for matrix elements, which can significantly speed the calculation, is lost.

THE O_2^+ ION

Semiempirical calculations on several states of O_2^+ were carried out by Bassani, Montaldi, and Fumi[24] al-

TABLE XIII. Calculated potential minima and vertical excitation energies for several states of O_2^{2+}.

State	r_e (Å)	E_{vert} (eV)
$^1\Sigma_g^+$	1.174	0.00
$^3\Sigma_u^+$	...	2.56
$^3\Delta_u$	...	5.07
$^3\Pi_g$	1.291	5.70
$^3\Sigma_u^-$	1.458	6.10
$^1\Sigma_u^-$	1.418	7.21
$^1\Pi_g^-$	1.271	7.26
$^1\Delta_u$	1.393	7.97
$^3\Delta_g$	...	8.41
$^3\Pi_u$	...	9.70
$^3\Sigma_g^-$	...	9.71
$^1\Pi_u$	...	10.69
$^1\Sigma_u^+$	...	12.04
$^1\Delta_g$	...	12.88
$^3\Sigma_g^+$	...	14.45
$^1\Sigma_g^-$	...	14.86

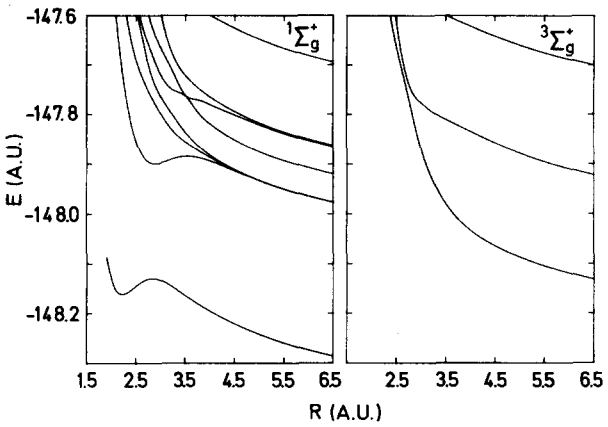

FIG. 19. Calculated $O_2^{2+\,1,3}\Sigma_g^+$ potential curves.

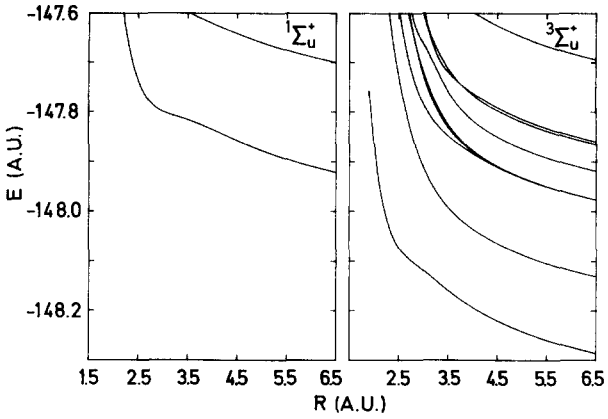

FIG. 21. Calculated $O_2^{2+\,1,3}\Sigma_u^+$ potential curves.

most 20 years ago. Later, Kotani and co-workers[25] performed *ab inito* CI calculations on four states of O_2^+ at an internuclear separation of 2.28167 a.u. using a minimum STO basis and 15 configurations. Dixon and Hull[26] used a semiempirical method with a fixed core in a CI calculation including all π electron configurations. They obtained partial potential curves for six states of $^2\Pi_u$, $^4\Pi_u$, and $^2\Phi_u$ symmetry. Newton and coworkers[27] calculated the bond length of the $X\,^2\Pi_g$ ground state, and Cade *et al.*[28] studied the electron distribution in this state. Raftery and Richards[29] calculated partial potential curves for several states of O_2^+ using Nesbet's open shell procedure including interaction between three configurations in the $^2\Pi_u$ case. The calculations of O_2^+ states were based upon Hartree–Fock results for $O_2(^3\Sigma_g^-)$ and $O_2(^1\Delta_g)$. Relative energies, vibrational frequencies, and equilibrium distances were calculated for seven states which may be seen in the photoelectron spectrum of $O_2(^1\Delta_g)$. Recently Jonathan *et al.*[30] obtained a ground state wavefunction for O_2^+ using a restricted open shell INDO-SCF procedure. This wavefunction was used for a calculation of vertical excitation energies for states of O_2^+ up to around 60 eV.

The 1*s* hole states of O_2^+ were studied by Bagus and Schaefer.[31] These states cannot be described by our method, which does not include configurations with 1*s* holes.

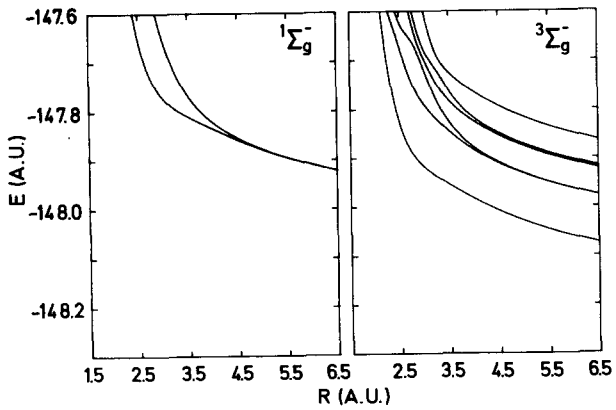

FIG. 20. Calculated $O_2^{2+\,1,3}\Sigma_g^-$ potential curves.

Very recently CI calculations not very different from ours have been carried out by Honjo, Tanaka, and Ohno.[32] Potential curves were obtained for nine states which may be observed in photoelectron spectra of O_2. The calculated vertical excitation energies are in good agreement with experiment.

The electronic states of O_2^+ have been studied extensively in a large number of experiments. Especially from photoelectron spectra of O_2 detailed information has been obtained for many of these states. In the review by Krupenie,[20] relative energies, some spectroscopic constants, and assignments are given for the following seven states: $X\,^2\Pi_g$, $a\,^4\Pi_u$, $A\,^2\Pi_u$, $b\,^4\Sigma_g^-$, $C\,^2\Delta_g$, $B\,^2\Sigma_g^-$, and $c\,^4\Sigma_u^-$. In the last few years, the amount of experimental information on these states has increased considerably, and in addition a $^2\Phi_u$ state around 7 eV above the $X\,^2\Pi_g$ ground state has been investigated in detail in photoelectron spectra on $O_2(^1\Delta_g)$ by Jonathan *et al.*,[30] and Samson and Petrosky.[33] The latter authors have also provided relatively accurate spectroscopic constants for the $C\,^2\Delta_g$ state. A state observed 12 eV (vertically) above the ground state has been tentatively assigned as $^2\Pi_u$ by Edqvist *et al.*,[34] and Gardner and Samson[35] from studies of photoelectron and photoion spectra.

A considerable number of higher states have been observed and tentatively assigned by Siegbahn *et al.*[36] and Jonathan[30] *et al.* These correspond to the following approximate relative energies (no spectroscopic constants have been found):

$^2\Sigma_u^-$(15.8 eV), $^2\Delta_u$(17.5 eV), $^2\Pi_u$(21.5 eV), $^4\Sigma_g^-$(27.5 eV)

$^2\Sigma_g^-$(29.5 eV), $^2\Sigma_g^+$(34.0 eV), $^4\Pi_u$(36.5 eV), $^2\Pi_u$(44.0 eV).

Also the much higher 1*s* hole states have been observed. Since these states hardly can be well described in a calculation of the present type, we have not attempted a comparison between our results and these measurements. In general, we find a high density of states in the region above 15 eV for all symmetries.

Also in the lower region the density of calculated states is high, and only a small fraction of the calculated states have been observed. This can be expected since many of the calculated states have large contri-

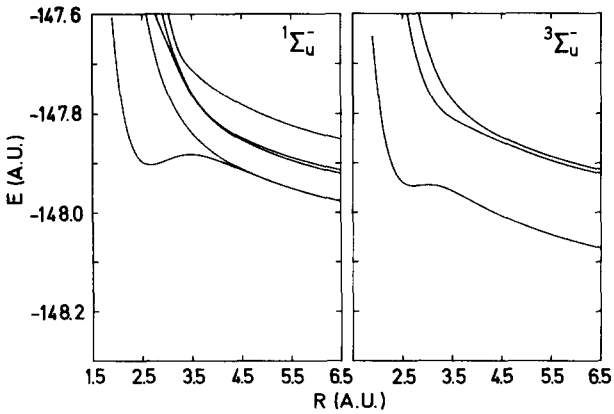

FIG. 22. Calculated O_2^{2+} $^{1,3}\Sigma_u^-$ potential curves.

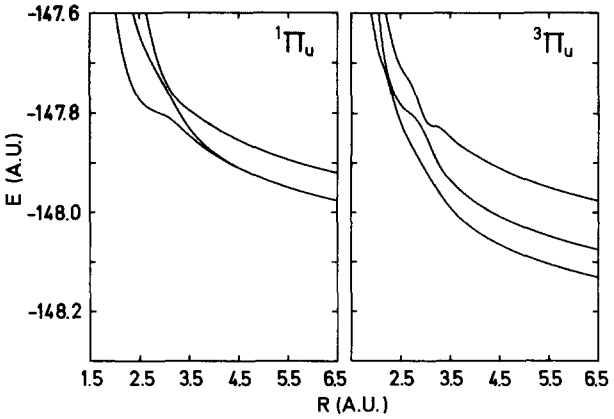

FIG. 24. Calculated O_2^{2+} $^{1,3}\Pi_u$ potential curves.

butions of multiply excited configurations, and therefore have small intensities in the photoelectron spectrum. Some of the states can only be reached from the metastable $^1\Delta_g$ state of O_2 as discussed by Raftery and Richards.[29] Such states include the $^2\Delta_g$ and $^2\Phi_u$ states, the assignments of which are confirmed by our calculations.

Tables VII–IX show the calculated and observed data, and the calculated potential curves are given in Figs. 9–18. The agreement for the seven states well-known from experiment is not quite as good as the similar agreement for the ions N_2^+ and NO^+.[4] On the other hand, the six excited states deviate in very much the same way. All calculated relative energies are too small by 0.6 to 1.3 eV (average deviation: 0.9 eV). The equilibrium distances are all too large by 0.02 to 0.04 Å (average deviation: 0.035 Å). The vibrational frequencies are too large by 80 to 250 cm^{-1} (maybe somewhat more for the $^2\Phi_u$ state for which ω_e has not been determined very accurately; from experiment the average deviation of the five well-known vibrational frequencies is 170 cm^{-1}). Finally, the dissociation energies are too large by 0.7 to 1.0 eV (average deviation: 0.85 eV). If orbital exponents for 2s and 2p STO's were chosen larger (more contracted basis) r_e would decrease, but ω_e and D_e would both increase. Lower values of ζ_{2s} and ζ_{2p} would have the opposite effect.

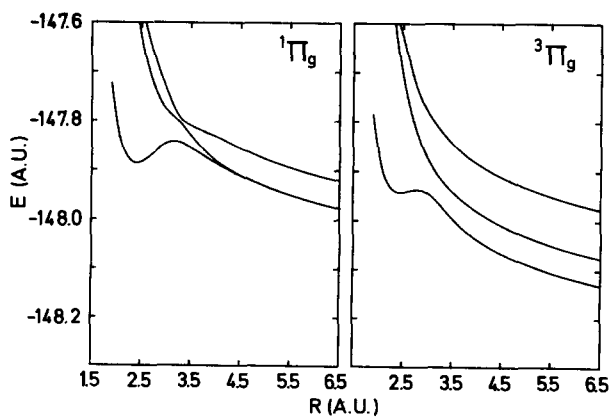

FIG. 23. Calculated O_2^{2+} $^{1,3}\Pi_g$ potential curves.

The systematic deviations can be used for improved predictions of the states which so far have not been observed or for which the experimental information is incomplete. This procedure may be less satisfactory for very shallow or very deep potential minima and in cases of avoided crossings, but we expect it to work well for other potential curves such as those for the six excited states that are well-known from experiment. The results obtained by this method for a large number of low-lying states are shown in Table X. From the results on the six known states we expect most of our predictions to be correct within ±0.4 eV for the relative energy, ±0.01 Å for r_e, ±100 cm^{-1} for ω_e and ±0.2 eV for D_e.

Among the individual potential curves that of the lowest $^4\Sigma_u^-$ state is of special interest. From the calculated shape (Fig. 12) it is easy to understand the fact that observations of different kinds have shown only the lowest one or two vibrational levels of this state ($c\,^4\Sigma_u^-$). This is the case both in photoelectron spectra (see, e.g., Edqvist *et al.*[34]) and in studies of the Hopfield bands ($c\,^4\Sigma_u^- - b\,^4\Sigma_g^-$, see e.g., LeBlanc[37]). The calculated r_e for $c\,^4\Sigma_u^-$ is 1.21 Å compared with $r_e = 1.28$ Å for the O_2 $X\,^3\Sigma_g^-$ ground state and $r_e = 1.32$ Å for $b\,^4\Sigma_g^-$ of O_2^+. The $c\,^4\Sigma_u^-$ curve has a second shallow minimum around $r_e = 1.8$ Å ($D_e \sim 0.5$ eV).

The calculated potential curves for the $^2\Pi_u$ states show besides the well-known $A\,^2\Pi_u$ state two bound states with relatively high dissociation energies [2.6 eV predicted for $^2\Pi_u(2)$ and 0.8 eV for $^2\Pi_u(3)$] and small equilibrium distances [predicted $r_e(^2\Pi_u(2)) = 1.4$ Å, $r_e[^2\Pi_u(3)] = 1.5$ Å. The calculated energies for the two curves for $R = 1.28$ Å (equilibrium distance for O_2 $X\,^3\Sigma_g^-$) are approximately 8 and 12 eV above the energy for the potential minimum of O_2^+ $X\,^2\Pi_g$. The observations of an intense vertical transition in the photoelectron spectrum around 24 eV (Edqvist *et al.*[34]) corresponding to 12 eV above the O_2^+ $X\,^2\Pi_g$ state can on the basis of energetic considerations thus be explained from the shape of the potential curve for $^2\Pi_u(3)$. This is in agreement with the assignment by Dixon and Hull,[26] who predicted that the transition to the state $^2\Pi_u(3)$ should have considerable intensity in the photoelectron spectrum. The transition to the $^2\Pi_u(2)$ state is predicted to have very low intensity.

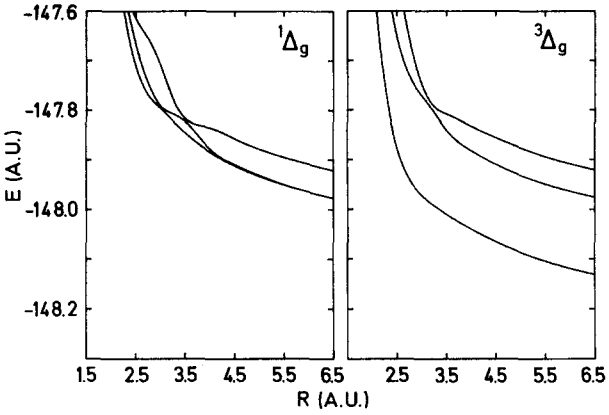

FIG. 25. Calculated O_2^{2+} $^{1,3}\Delta_g$ potential curves.

From our calculations (Fig. 14) we expect the transition to occur as a long vibronic series with an intensity distribution like that for the $A\,^2\Pi_u$ state (the $A\,^2\Pi_u$ and $^2\Pi_u(2)$ potential curves are almost parallel). The intensity maximum should be around 20 eV in the photoelectron spectrum.

The observation of an intense continuous absorption around 27 eV in the photoelectron spectrum (15 eV above the O_2^+ $X\,^2\Pi_g$ ground state) by Edqvist *et al.*[34] and other workers might from an energy criterion alone correspond to a vertical transition to $^2\Sigma_g^+(2)$, $^4\Sigma_g^+(1)$, $^4\Sigma_g^-(2)$, $^6\Sigma_u^+(1)$, $^2\Sigma_u^-(2)$, $^4\Sigma_u^-(2)$, $^2\Pi_g(3)$, $^4\Pi_u(2)$, $^2\Delta_u(2)$, and $^2\Phi_g(1)$. Of these only the $^6\Sigma_u^+(1)$, $^2\Delta_u(2)$, and $^2\Phi_g(1)$ states can be excluded from simple intensity considerations, and the absorption may be due to several of the above mentioned states, including the $^2\Sigma_u^-$ state as suggested by Siegbahn *et al.*[36]

THE O_2^{2+} ION

The O_2^{2+} ion has been observed in electron impact experiments by Dorman and Morrison[38] and later by Daly and Powell.[39] They found that the ground state $X\,^1\Sigma_g^+$ has an energy around 37 eV above the O_2 $X\,^3\Sigma_g^-$ ground state, a much lower value than those predicted earlier. Daly and Powell also found a state of O_2^{2+} 4 eV higher; this was assigned to a $^3\Sigma_u^+$. Auger spectroscopy measurements by Moddeman *et al.*[40] showed several states of O_2^{2+}, among these the ground state $X\,^1\Sigma_g^+$ (38 eV vertically above the O_2 $^3\Sigma_g^-$ ground state), a state assigned to $a\,^3\Sigma_u^+$ (around 43 eV) and one assigned to $c\,^3\Pi_u$ (around 51 eV). The double charge transfer measurements by Appell *et al.*[41] showed two states that were assigned to $b\,^3\Pi_g$ or $b'\,^3\Sigma_u^-$(43 eV) and $c\,^3\Pi_u$(48 eV). According to the empirical model by Hurley[42] there are several additional states below 50 eV. These are primarily singlet states and have not been observed yet.

The results of the present calculations are shown in Tables XI–XIII and Figs. 19–26. The energies are given relative to the O_2^{2+} $X\,^1\Sigma_g^+$ ground state. The number of low-lying states is very high, and some of them have not been predicted by Hurley because of lack of information on the corresponding state of the isoelectronic system N_2. Our calculations confirm that the ground state is $^1\Sigma_g^+$, and the lowest excited state $^3\Sigma_u^+$. This state is found to be only 2.6 eV above $X\,^1\Sigma_g^+$, considerably less than predicted by experiment. The $a\,^3\Sigma_u^+$ state is predicted not to have a potential minimum, whereas the ground state minimum is found at r_e = 1.174 Å, very close to the value calculated for the corresponding state of the isoelectronic molecule N_2. The calculations predict a new state, $^3\Delta_u$, below the $^3\Pi_g$ state, for which the assignment by Appell *et al.*[41] is confirmed. The $^3\Pi_g$ state and the following four states $^3\Sigma_u^-$, $^1\Sigma_u^-$, $^1\Pi_g$, and $^1\Delta_u$ are all found to have potential minima. The observation by Appell *et al.*[41] of a state around 10 eV above the ground state might be due to the $^3\Pi_u$ or $^3\Sigma_g^-$ state. The observation of a state around 13 eV by Moddeman *et al.*[40] may be due to a transition to one of the higher states in Table XIII and probably not as suggested to the $^3\Pi_u$ state.

In general, the relative energies should be used with caution in the assignments, since among other things the steep shape of the O_2^{2+} potential curves in the region of interest makes very precise predictions impossible.

It has long been experienced that minimal basis VCI calculations tend to give r_e values which are too large, while SCF calculations tend to predict too small values. Thus Hopkinson *et al.*[43] obtained r_e = 1.034 Å from a double-zeta SCF calculation on the $X\,^1\Sigma_g^+$ state, while we find r_e = 1.174 Å. We expect that our calculated values in Table XIII are almost certainly too large, for Hurley's empirical values obtained by comparison with the isoelectronic N_2 states tend to be more than 0.1 Å lower than ours. It is worth noting that Hurley predicted bound $^3\Sigma_u^+$ and $^3\Pi_u$ states with effective dissociation energies around 0.5 eV. Our calculations do not show any potential minima for these states.

CONCLUSION

It has been shown that the VCI method gives results in reasonably good agreement with experiment for a large number of states of the neutral O_2 molecule and the ion O_2^+. The use of a minimal basis, which is essential for limiting the number of configurations in a

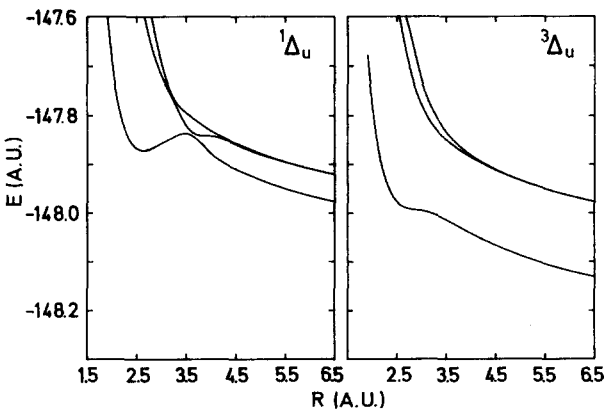

FIG. 26. Calculated O_2^{2+} $^{1,3}\Delta_u$ potential curves.

non *ad hoc* way, does allow a description of most low-lying non-Rydberg states which is useful for many purposes. The deviations from experiment in the depth and position of the curves are usually reasonably small and tend to be rather regular, enabling corrections to be made to allow predictions about states for which no experimental information is yet available. Thus we are able to obtain a considerable amount of information especially about the oxygen ions which should prove useful in interpretation of experimental data on these systems.

Note added in proof: We have recently been informed [J. Durup, Université de Paris (private communication)] that a $^4\Pi_g$ state has been observed in laser crossed beam photodissociation experiments.

ACKNOWLEDGMENTS

This work was supported by Statens Naturvidenskabelige Forskningsråd. Grants of computer time from the Regional Data Center of Aarhus University are gratefully acknowledged.

[1]G. J. Schulz, Rev. Mod. Phys. 45, 423 (1973).
[2]H. H. Michels and F. E. Harris, *Electronic and Atomic Collisions Abstracts* (North-Holland, Amsterdam, 1971), p. 1170; M. Krauss, D. Neumann, A. C. Wahl, G. Das, and W. Zemke, Phys. Rev. A 7, 69 (1973).
[3]J. Kouba and Y. Öhrn, J. Chem. Phys. 52, 5387 (1970).
[4]E. W. Thulstrup and A. Andersen, J. Phys. B 8, 965 (1975).
[5]E. Clementi and D. C. Raimondi, J. Chem. Phys. 38, 2686 (1963).
[6]W. J. Stevens, G. Das, A. C. Wahl, M. Krauss, and D. Neumann, J. Chem. Phys. 61, 3686 (1974).
[7]See NAPS document 2726 for 60 pages of supplementary material. Order from ASIS/NAPS, c/o Microfiche Publications, 440 Park Avenue South, New York, N. Y. 10016. Remit in advance for each NAPS accession number $1.50 for microfiche or $5.00 for photocopies up to 30 pages, $0.15 for each additional page. Make checks payable to Microfiche Publications. Outside of the U. S. and Canada, postage is $2.00 for a photocopy and $0.50 for a microfiche.
[8]J. H. Ahlberg, E. N. Nilson, and J. L. Walsh, *The Theory of Splines and Their Applications* (Academic, New York, 1967).
[9]J. L. Dunham, Phys. Rev. 41, 721 (1932).
[10]Y. P. Varshni, Rev. Mod. Phys. 29, 664 (1957).
[11]D. Steele, E. R. Lippincott, and J. T. Vanderslice, Rev. Mod. Phys. 34, 239 (1962).
[12]H. M. Hulburt and J. O. Hirschfelder, J. Chem. Phys. 9, 61 (1940).
[13]R. N. Zare, J. Chem. Phys. 40, 1934 (1964).
[14]F. J. Zeleznik, J. Chem. Phys. 42, 2836 (1965).
[15]J. Tellinghuisen, Comp. Phys. Commun. 6, 221 (1974).
[16]M. Krauss, Nat. Bur. Stand. Tech. Note USA 438 (1967).
[17]W. G. Richards, T. E. H. Walker, and R. K. Hinkley, *A Bibliography of ab initio Molecular Wave Functions* (Clarendon, Oxford, 1971).
[18]W. G. Richards, T. E. H. Walker, L. Farnell, and P. R. Scott, *Bibliography of ab initio Molecular Wave Functions, Supplement for* 1970-1973 (Clarendon, Oxford, 1974).
[19]H. F. Schaefer III and F. E. Harris, J. Chem. Phys. 48, 4946 (1968).
[20]P. H. Krupenie, J. Phys. Chem. Ref. Data 1, 423 (1972).
[21]H. F. Schaefer III, J. Chem. Phys. 54, 2207 (1971).
[22]H. F. Schaefer III and W. H. Miller, J. Chem. Phys. 55, 4107 (1971).
[23]S. D. Peyerimhoff and R. J. Buenker, Chem. Phys. Lett. 16, 235 (1972).
[24]F. Bassani, E. Montaldi, and F. G. Fumi, Nuovo Cimento 3, 893 (1956).
[25]M. Kotani, Y. Mizuno, K. Kayama, and E. Ishiguro, J. Phys. Soc. Jpn. 12, 707 (1957).
[26]B. N. Dixon and S. E. Hull, Chem. Phys. Lett. 3, 367 (1969).
[27]M. D. Newton, W. A. Lathan, W. J. Hehre, and J. A. Pople, J. Chem. Phys. 52, 4064 (1971).
[28]P. E. Cade, R. F. W. Bader, and J. Pelletier, J. Chem. Phys. 54, 3517 (1971).
[29]J. Raftery and W. G. Richards, Int. J. Mass. Spectrom. Ion Phys. 6, 269 (1971).
[30]N. Jonathan, Faraday Discuss. Chem. Soc. 54, 67 (1972); N. Jonathan, A. Morris, M. Okuda, K. J. Ross, and D. J. Smith, Faraday Discuss. Chem. Soc. 54, 48 (1972); J. Chem. Soc. Faraday II 70, 1810 (1974).
[31]P. S. Bagus and H. F. Schaefer III, J. Chem. Phys. 56, 224 (1972).
[32]N. Honjo, K. Tanaka, and K. Ohno, in Progress Report No. VIII from Research Group on Atoms and Molecules, Ochanomizu University, Tokyo, Japan, 1975.
[33]J. A. R. Samson and V. E. Petrosky, J. Electron Spectrosc. Relat. Phenom. 3, 461 (1974).
[34]O. Edqvist, E. Lindholm, L. E. Selin, and L. Åsbrink, Phys. Scripta 1, 25 (1970).
[35]J. L. Gardner and J. A. R. Samson, J. Chem. Phys. 62, 4460 (1975).
[36]K. Siegbahn, C. Nordling, G. Johansson, J. Hedman, P. F. Heden, K. Hamrin, U. Gelius, T. Bergmark, L. O. Werme, R. Manne, and Y. Baer, *ESCA Applied to Free Molecules* (North-Holland, Amsterdam, 1969).
[37]F. J. Leblanc, J. Chem. Phys. 38, 487 (1963).
[38]F. H. Dorman and J. D. Morrison, J. Chem. Phys. 39, 1906 (1963).
[39]N. R. Daly and R. E. Powell, Proc. Phys. Soc. (London) 90, 629 (1967).
[40]W. E. Moddeman, T. A. Carlson, M. O. Krause, B. P. Pullen, W. E. Bull, and G. K. Schweitzer, J. Chem. Phys. 55, 2317 (1971).
[41]J. Appell, J. Durup, F. C. Fehsenfeld, and P. Fournier, J. Phys. B 6, 197 (1973).
[42]A. C. Hurley, J. Mol. Spectrosc. 9, 18 (1962).
[43]A. C. Hopkinson, K. Yates, and I. G. Csizmadia, Theor. Chim. Acta 23, 369 (1972).